THE JOURNAL OF PHYSICAL CHEMISTRY B

Article

Cite This: J. Phys. Chem. B 2018, 122, 10855−10860

pubs.acs.org/JPCB

An NMR Confirmation for Increased Folded State Entropy Following Loop Truncation

Yulian Gavrilov,*,† Shlomi Dagan,‡ Ziv Reich,‡ Tali Scherf,*,§ and Yaakov Levy*,†

†Department of Structural Biology, ‡Department of Biomolecular Sciences, and §Department of Chemical Research Support, Weizmann Institute of Science, Rehovot 76100, Israel

Supporting Information

ABSTRACT: Previous studies conducted on flexible loop regions in proteins revealed that the energetic consequences of changing loop length predominantly arise from the entropic cost of ordering a loop during folding. However, in an earlier study of human acylphosphatase (hmAcP) using experimental and computational approaches, we showed that thermodynamic stabilization upon loop truncation can be attributed mainly to the increased entropy of the folded state. Here, using ^{15}N NMR spectroscopy, we studied the effect of loop truncation on hmAcP backbone dynamics on the picosecond−nanosecond timescale with the aim of confirming the effect of folded state entropy on protein stability. NMR-relaxation-derived N−H squared generalized order parameters reveal that loop truncation results in a significant increase in protein conformational flexibility. Comparison of these results with previously acquired all-atom molecular dynamics simulation, analyzed here in terms of squared generalized NMR order parameters, demonstrates general agreement between the two methods. The NMR study not only provides direct evidence for the enhanced conformational entropy of the folded state of hmAcP upon loop truncation but also gives a quantitative measure of the observed effects.

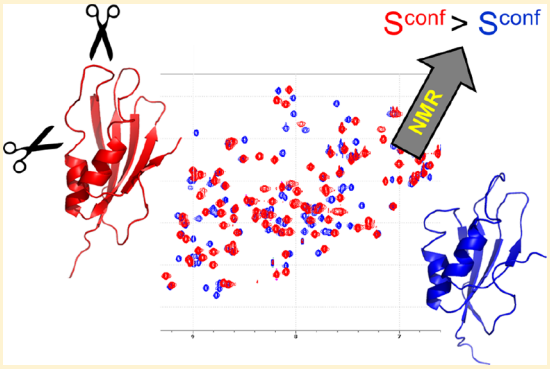

INTRODUCTION

Changes in native state conformational dynamics can affect protein function significantly. Conformational heterogeneity and dynamics play an important role in protein−ligand binding[1−5] and allostery,[6] and should be explicitly considered in protein evolution and design.[7] Structured loops in proteins usually possess a high level of conformational flexibility, which is often related to their function.[8] Loops can adopt specific conformations, for example, to assist protein recognition.[9−12] In addition to their connecting and functional roles, flexible regions can affect the kinetics and thermodynamics of the whole protein.

Previously it was shown that loop length variation can affect protein thermodynamic stability. This effect is mostly related to the entropic cost of ordering a loop on folding.[13−17] An unfolded state ensemble of proteins with shorter loops has lower configurational entropy (i.e., smaller entopic cost for loop closure), and thus greater thermodynamic stability. However, in our recent studies using computational and experimental tools, we demonstrated that shortening the length of the loop can substantially affect protein stability by increasing the protein's native state entropy,[18,19] in addition to its effect on the unfolded state, as predicted by the entropic cost of loop closure. Specifically, we showed that deletion of two, four and six residues from the L4 loop of human muscle acylphosphatase (hmAcP) results in gradual thermal and chemical stabilization of the protein. This effect can be quite significant, with the deletion of six residues (S71, P72, S73, S74, R75, I76) resulting in ∼2 kcal/mol stabilization of the Δ6 mutant relative to the wild type (WT) protein.[18] Notably, calorimetric measurements showed that unfolding enthalpy decreases substantially upon loop truncation. This decrease opposes the measured change in conformational stability of the proteins, which, as mentioned above, increases as the loop becomes shorter.[18] Furthermore, the truncation had only a very small effect on the folding rate of the protein but led to a marked decrease of the unfolding rate. These features cannot be explained solely by contribution decrease in loop closure entropy and indicate that the stabilization of hmAcP upon loop shortening is related, at least in part, to the properties of the folded state.

Indeed, using molecular dynamics (MD) simulations, we demonstrated that shortening the L4 loop leads to an increase in the entropy of the folded state, which stabilizes the proteins by decreasing the entropic gain of unfolding.[18] We further showed that this entropic effect arises from an increased flexibility of both the backbone and side chains. In order to generalize the effect of loop length shortening on the conformational entropy of the native state, we subsequently studied this effect in three other proteins: ubiquitin

Received: October 3, 2018
Revised: November 4, 2018
Published: November 9, 2018

DOI: 10.1021/acs.jpcb.8b09658
J. Phys. Chem. B 2018, 122, 10855−10860

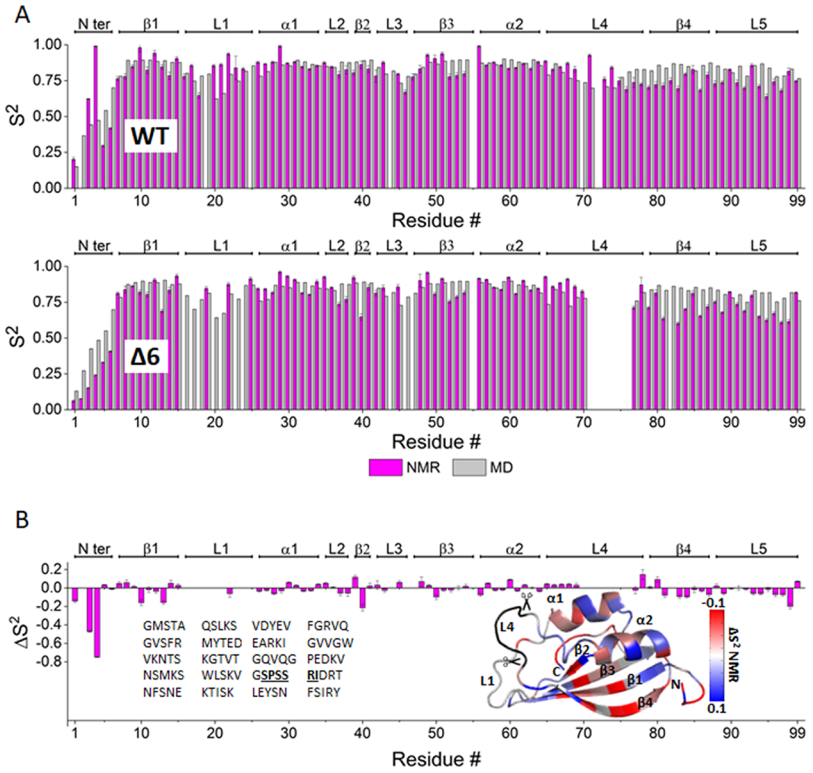

Figure 1. (A) Squared generalized order parameters for backbone N−H groups (S^2) derived from NMR (magenta) and MD (gray) data for the WT (upper panel) and the truncated Δ6 variant (lower panel) of the hmAcP protein. (B) The difference in NMR-derived squared generalized order parameters between the truncated and WT variants: $\Delta S^2 = S^2(\Delta 6) - S^2(\mathrm{WT})$. The borders of the structural elements are depicted at the top of each spectrum. Insertions: The structure of the hmAcP protein showing ΔS^2 per residue. The color scale is from −0.1 (red) to 0.1 (blue). Truncated residues in L4 (Δ6) are shown in black; the borders of the truncated region are indicated by the scissors sign. The homology model of hmAcP is based on the solution structure of the horse orthologue of hmAcP (PDB code: 1APS); hmAcP sequence (truncated residues are in bold and underlined).

conjugation E2 enzyme Ubc7, and two circular permutants of the α-spectrin SH3 domain, in which we gradually deleted residues in selected loops (two, four or six residues in hmAcP and Ubc7, and two or four residues in the SH3 permutants) and quantified the dynamics of the WT and the loop-shortened variants.[19] Using all-atom MD, we found that an increase in the native state entropy following loop shortening is not unique to hmAcP, yet nor is it a general consequence of loop truncation. It still remains unclear which loops, upon shortening, are expected to exhibit this effect on conformational entropy.

Squared generalized NMR order parameters (hereafter NMR order parameters, S^2), which can be derived from relaxation experiments, describe the amplitudes of motion on the fast picosecond−nanosecond timescale and can be used to estimate the conformational entropy of a protein. Here, we directly experimentally characterized the effect of loop truncation on hmAcP backbone dynamics on the picosecond−nanosecond timescale by ^{15}N NMR relaxation. We focus on quantification of the conformational dynamics of the backbone because it is expected to be affected by the loop truncation. Side-chain dynamics, which is not strictly coupled to backbone dynamics, obviously contributes to the conformational entropy of the native state.[20] While the side-chain entropy in the folded state is expected to be affected, for example, upon ligand binding,[21−23] loop truncation is expected to have a larger effect on the backbone dynamics. Large change in backbone entropy was also observed for some proteins upon ligand binding.[24−26] Measuring backbone entropy can therefore capture the effect of truncation on protein stability, but complete quantification may demand estimation of the sidechain entropy.

METHODS

The relaxation experiments were performed on the WT and the Δ6 variant at two magnetic field strengths, 14.1 and 18.8 T, at 293 K. hmAcP protein, which is a small 99 residue enzyme that catalyzes the hydrolysis of the carboxyl−phosphate bond in various acylphosphate compounds and presents an open α/β-sandwich structure,[27] was studied previously in solution using NMR by Fusco et al., who assigned ^{1}H, ^{13}C and ^{15}N resonances for the WT protein.[28] The 3D NMR-derived solution structure has, however, been determined only for the horse orthologue of hmAcP.[29] This protein differs from hmAcP in only five amino acids, all of which are located outside of the truncated L4 region. This structure was formerly used by us to generate homology models of WT and Δ6 hmAcP. The two helices (α1, α2) of the protein run almost parallel to each other; the main chain geometry of antiparallel β sheet is quite regular. The two helices pack closely onto the β sheet with the helix axes parallel to the strands of the sheet.[29] L1 loop connects α1 with β1 and L4 connects α2 with β4 (Figure 1, insertion).

To track the residue-specific dynamics of N−H bond vectors of the WT hmAcP protein and its Δ6 variant, ^{1}H−^{15}N correlations in the corresponding ^{15}N heteronuclear single-quantum coherence (HSQC) NMR spectra were assigned using multidimensional triple resonance NMR techniques, and

DOI: 10.1021/acs.jpcb.8b09658
J. Phys. Chem. B 2018, 122, 10855−10860

^{15}N,^{13}C-labeled samples (see Materials and Methods in Supporting Information). Assignment of the WT protein was verified by comparing the assignments to those made by Fusco et al. at 298 K.[28] In total, 96 out of 97 non-proline residues were unambiguously assigned for WT hmAcP and considered in further dynamics analysis. Similarly to the previous study,[28] the solvent-exposed G70 signal was not observed in the HSQC NMR spectrum.

RESULTS AND DISCUSSION

Previous far-UV circular dichroic and fluorescence emission spectra revealed no major changes in hmAcP structure upon L4 loop truncation.[18] NMR spectroscopy reveals that, for most residues, the observed ^{1}H, ^{15}N chemical shifts of the WT and Δ6 mutant are similar. The differences in ^{1}H, ^{15}N chemical shifts between WT and Δ6 (ΔCS, Supporting Information) are presented in Figure S1. Changes in chemical shift reflect changes in the chemical environment, which are expected for those Δ6 residues in the vicinity of the truncated region. Many of the Δ6 residues whose N−H HSQC correlation signal significantly changes position (ΔCS > 0.50 ppm) are indeed located close to the truncation site, being either sequentially (S67, K68, V69, and D77) or spatially (S22, Y26, T27, and S96) neighboring residues therein. Other residues that exhibited significant change in their chemical shifts (V18, D29, and V48) are located in parts of the protein that directly interact with the truncated L4 residues and may experience changes in their local environment. For N- and C-terminal residues, M1 and S96 (ΔCS > 1.00 ppm) MD simulations revealed a noticeable change in the relative position of these terminal residues in Δ6.[19] Serine 82 is also characterized by a very high ΔCS value (1.58 ppm). This large change in the chemical environment could be related to changes in the strength of the hydrogen bond interaction between its N−H group and backbone oxygen of D11 in neighboring beta strand. For Δ6, residues R17, V21, F23, and G46, which are located in flexible regions of the protein,[19] were not observed in the NMR spectra. Therefore, out of the 92 non-proline residues, 88 were considered in further dynamics analysis.

The picosecond−nanosecond timescale conformational dynamics of WT and Δ6 hmAcP were studied using the Lipari−Szabo model-free (MF) formalism, including its extended form.[30−33] Squared generalized order parameters, S^2 derived by this method, are typically interpreted as amplitudes of picosecond−nanosecond local motions. As such, S^2 may be used to estimate the contribution of a particular relaxation probe (N−H bond, in this case) to the conformational entropy of a protein.[34−36] ^{15}N R_1, R_2 and heteronuclear NOE data were fit on a per-residue basis using the five MF motional models (MF 1−5).[37] Since the ratio between parallel and perpendicular components ($D_{\parallel}/D_{\perp}$) of the rotational diffusion tensor which describes the overall tumbling of a molecule is quite high for Δ6 (1.38), we assumed an anisotropic tumbling. Our motivation was to compare the backbone dynamics for each residue in the WT and in Δ6, thus the final choice of the model was based on how well it fits each N−H group in both proteins. The optimized MF parameters for the analyzed residues are presented in Tables S1 and S2. Although in the case of WT hmAcP, 96 non-proline residues were unambiguously assigned, the peaks of residues S2, Q19, M25, and S44 were too weak to be observed in the NMR relaxation experiments. For Δ6, the peaks of residues G16, V18, G20, R24, S44, T47 and S82 were either too weak (line broadening) or their relaxation parameters could not be fitted. In total, the picosecond−nanosecond conformational dynamics comparative study comprised 77 residues (out of 92 non-proline residues that are identical in the WT and Δ6) for which NMR relaxation data for both hmAcP proteins were available. The values of NMR-derived backbone order parameters were in the range of 0.20−0.99 for WT and 0.06−0.96 for Δ6 (Figure 1A); weighted mean values were 0.82 ± 0.14 (WT) and 0.67 ± 0.12 (Δ6). The greater order parameters for WT than Δ6 is further illustrated by the derived weighted pairwise root-mean-square deviation (rmsd)[5] which equals 0.10 (see Materials and Methods in Supporting Information). The values above are given without considering the A4 residue (see discussion below). Further, exclusion of five N-terminal and five C-terminal residues from these calculations still results in higher values for WT: weighted mean values are 0.84 ± 0.13 (WT) and 0.76 ± 0.12 (Δ6). These values suggest that the observed difference in the order parameters cannot be explained solely by the terminal effects. In general, these values indicate that, consistent with our previous findings,[18,19] truncation of L4 significantly increases the overall flexibility of hmAcP, manifested here as a decrease in backbone order parameters.

Backbone N−H group order parameters were extracted from previously acquired 2−2.5 μs MD simulations of WT and Δ6 hmAcP,[19] using the iRED method.[38] The latter relies on a principal component analysis of the isotropically averaged covariance matrix of the lattice functions of the spin interactions responsible for spin relaxation (dipolar interactions and chemical shift anisotropy).[38] The values obtained were compared with the NMR-derived experimental data (Figure 1A; for details see Materials and Methods in Supporting Information). For the MD-derived order parameters, weighted mean values were 0.86 ± 0.002 (WT) and 0.86 ± 0.003 (Δ6); the weighted pairwise rmsd was 0.02. Thus, the simulations do not show any change in average S^2 values. A per-residue comparison of the NMR and MD-derived backbone order parameters (S^2) revealed low correlation between the values derived for the two proteins (R^2 < 0.40). However, at the level of secondary structures (where S^2 denotes the sum per secondary structural element) the correlation became much higher: R_{WT}^2 = 0.87 and $R_{\Delta 6}^2$ = 0.85 (see also Figure S2). Thus, although there are some differences in S^2 at the residue level between WT and Δ6, the two methods exhibit the same trends along the sequence. This level of similarity between the NMR and MD data for the backbone N−H order parameters is relatively good. The correlation between experimentally and computationally measured order parameters is often lower than 0.8.[39] While several studies showed good agreement between entropy measured from NMR and MD simulations,[20,40] an improvement in MD force-fields is needed in more properly representing side-chain flexibility and in achieving extensive sampling of backbone dynamics to further increase the correlation.[38,41,42]

A per-residue analysis of the difference in NMR-derived order parameters, ΔS^2 (the difference between the S^2 values of Δ6 and WT hmAcP) (Figure 1B) reveals which parts of the protein are mostly affected by the truncation of the L4 loop. The most pronounced effect is observed for the N-terminal region of the protein, where the backbone dynamics of resides M1, T3, and A4 are significantly increased upon loop truncation. This region is quite far from the L4 loop but is

DOI: 10.1021/acs.jpcb.8b09658
J. Phys. Chem. B 2018, 122, 10855−10860

connected to the β1 strand, through several residues that are also significantly affected by the truncation. The β1 strand continues into the L1 loop, which is located above the L4 loop. Our previous studies showed that L1 forms many contacts with L4, including with residues in the truncated region (G20−S74, G20−R75, G20−I76, V21−S75, V21−R75, V21−I76; S22−P72, S22−S73, S22−S74, S22−I76, F23−S76, R24−P72, M25−P72). The loss of most of those contacts upon truncation may affect proximate regions and disrupt the contacts between α1 and the end of L4, between L4 and L1, and between L4 and L3, thereby increasing the overall flexibility of the angle between the α1 and α2 helices (see ref 19 for further details). We note that residue A4 exhibits an especially large increase in N−H flexibility (ΔS^2 = −0.75). However, because the relaxation data for A4 in WT was not fitted well with any of the MF models (χ^2 > 1000), we excluded its contribution from further analysis.

Out of fifteen residues that are not observed in the NMR picosecond−nanosecond dynamics analysis (of WT and/or Δ6) nine belong to the L1 loop, including its C-terminal helix-like segment (G16−M25, excluding S22). To probe the presence of slow motions and hence check if these residues are related to microsecond−millisecond exchange line-broadening, we performed an ^{15}N relaxation dispersion experiment[43−45] for Δ6. However, the relaxation dispersion curves (data not shown) did not show a significant Carr−Purcell−Meiboom−Gill field dependence, which indicates the absence of noticeable slow timescale dynamics for the L1 loop (see Materials and Methods in Supporting Information).

The per-residue difference in the backbone order parameters for the middle regions of the hmAcP sequence (from α1 to α2) upon loop truncation is quite diverse and varies significantly from residue to residue, even within the same secondary structural element. In general, residues close to the truncated part exhibit systematically decreasing backbone flexibility. At the beginning of the L4 loop and after the Δ6 deleted region, three residues have positive ΔS^2 values. This is expected since the truncation decreases the conformational space accessible to the elements connected to the removed segment (the remaining of L4 and the beginning of β4). In contrast to the residues close to the truncation site, residues in the rest of β4 and in the C-terminal L5 systematically present increased backbone conformational flexibility (with a few exceptions). This was also indicated in our computational study and may be related to the significant change in the positions of these residues in Δ6.[19] In contrast to other L5 residues, C-terminal Y99 is characterized by a small positive ΔS^2 value. This effect may be related to the spatial proximity of Y99 to W39, which is also characterized by the positive ΔS^2 value. According to the homology model of hmAcP, the sidechains of these residues can form a π-stacking interaction. Even slight changes in their relative orientation in Δ6 may increase the strength of this interaction and decrease conformational flexibility in this region of the protein.

To obtain a quantitative measure of the observed effects, we estimated the entropic effect of the truncation of hmAcP L4 loop. The change in conformational entropy upon protein modifications or binding can be estimated from the order parameters.[35,36,46] In our case, we used the dictionary approach developed by Li and Bruschweiler to obtain entropy from NMR order parameters.[46] This approach interprets entropy derived from order parameters in terms of dihedral angle dynamics. In addition, we estimated the conformational entropy of the studied systems from MD simulations using distributions of the backbone dihedral angles[5,47−54] (see Materials and Methods in Supporting Information). The distributions of $T\Delta S^{NMR}_{backbone}$ and $T\Delta S^{MD}_{backbone}$, summed over each secondary structural elements, are presented on the homology model of hmAcP (Figure 2). At the level of the secondary

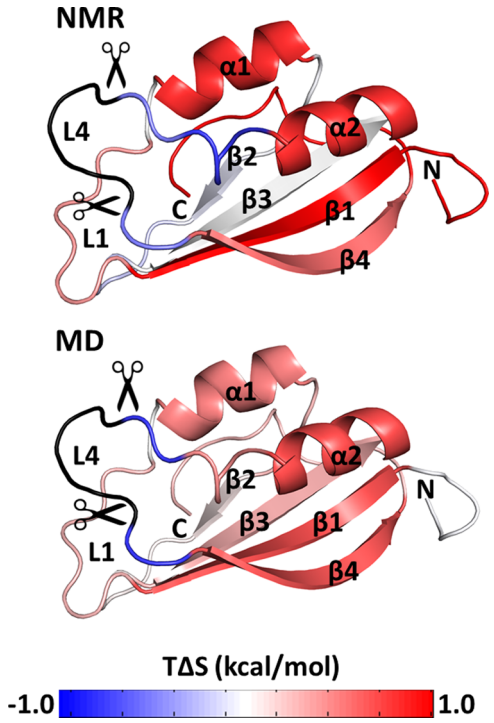

Figure 2. Difference in entropic contribution ($T\Delta S$, kcal/mol) between Δ6 and WT hmAcP. The color scale is from −1 (blue) to 1 (red) kcal/mol. The values are presented as the sum per structural element for NMR-based (top) and MD-based (bottom) data. Truncated residues in L4 (Δ6) are shown in black; the boarders of the truncated region are indicated by the scissors sign. The homology model of hmAcP is based on the solution structure of the horse orthologue of hmAcP (PDB code: 1APS).

structures, $T\Delta S$ values derived from MD compare well with those determined by NMR, with one exception regarding the conformational flexibility of the N-terminal region.

Overall, the two approaches agree that the increased entropy of Δ6 folded state is a global effect rather than one localized to the truncation site. The difference in entropic contributions from backbone atoms derived from the NMR experiments is $T\Delta S^{NMR}_{backbone}$ = 3.80 ± 0.11 kcal/mol whereas that derived from the MD simulations is $T\Delta S^{MD}_{backbone}$ = 3.35 ± 0.90 kcal/mol, remarkably close to the experimentally-derived value. The estimated increase in sidechain entropy of Δ6 compared to the WT is $T\Delta S^{MD}_{sidechains}$ = 3.88 ± 1.17 kcal/mol, which is similar to increase in backbone entropy. The total change in entropic contributions (backbone and sidechains) to the stability of the folded state between the WT and Δ6 is thus 7.60 ± 0.50 kcal/mol. According to our previous experimental data, the difference in entropic contributions to the overall thermodynamic stability between the two proteins is 14.90 ± 0.56 kcal/mol.[18] According to the same study, changes in folded state entropy upon loop truncation should amount to about 60% of this value (~8.90 kcal/mol). Based on these estimates, the difference between NMR-derived folded state $T\Delta S$ and

DOI: 10.1021/acs.jpcb.8b09658
J. Phys. Chem. B 2018, 122, 10855−10860

previously obtained experimental data is about 1.5 kcal/mol. We note that fifteen residues were not observed in the NMR picosecond−nanosecond dynamics analysis. The derivation of $T\Delta S$ from S^2 is based on the assumption that the orientations of the bond vectors are statistically independent of other degrees of freedom of the molecule,[35] which is not always the case.[55] Moreover, it was shown that correlation in fluctuations of flanking and non-flanking backbone torsion angles may lead to overestimation of conformational entropy.[26] To check this possibility, we used an alternative approach, developed by Sharp et al.[26] in order to estimate the difference in entropic contributions from backbone atoms derived from the NMR experiments and MD simulations. Although, the obtained values ($T\Delta S^{NMR}_{backbone}$ = 3.34 ± 0.26 kcal/mol; $T\Delta S^{MD}_{backbone}$ = 1.99 ± 0.01 kcal/mol) are not identical to the values calculated using distributions of the backbone dihedral angles, they too lead to the same conclusions.

CONCLUSIONS

The results presented here correlate well with the previously suggested mechanism of entropic stabilization of hmAcP upon shortening a long loop.[18] The greater backbone conformational entropy upon loop truncation is reminiscent to the increased backbone entropy observed by NMR upon binding of hydrophobic ligand.[25] Future study will quantify by NMR the contribution of sidechain flexibility to the increased entropy due to the loop truncation. The consistency between the NMR and MD simulations supports our previous computational analysis of changes in folded state conformational dynamics in the truncated proteins.[18,19] Finally, the NMR-derived data presented in this study provide direct experimental support for the notion that protein thermodynamics can be modulated not only by the enthalpy of the folded state but also via its entropy.[18,19,56]

ASSOCIATED CONTENT

Supporting Information

The Supporting Information is available free of charge on the ACS Publications website at DOI: 10.1021/acs.jpcb.8b09658.

Materials and Methods; Tables S1 and S2; Figures S1 and S2 (PDF)

AUTHOR INFORMATION

Corresponding Authors

*E-mail: yulian.gavrilov@gmail.com (Y.G.).
*E-mail: Tali.Scherf@weizmann.ac.il (T.S.).
*E-mail: Koby.Levy@weizmann.ac.il. Phone: 972-8-9344587 (Y.L.).

ORCID

Yaakov Levy: 0000-0002-9929-973X

Author Contributions

Y.L. and T.S. conceived the study and designed the research. S.D. performed the research; Y.G., T.S. performed the research and analyzed data. Y.G., Z.R., T.S., and Y.L. wrote the manuscript.

Notes

The authors declare no competing financial interest.

ACKNOWLEDGMENTS

We thank Drs. Shira Albeck, Yoav Peleg, Jossef Jacobovitch, and Ada Dantes (Israel Structural Proteomic Center, Weizmann Institute of Science) for their help in producing the proteins used in this study; we are grateful for Dr. Wolfgang Bermel (Bruker Biospin GmbH) for his help with Dynamics Center, and to Prof. Eva Meirovitch and Dr. Rina Rosenzweig for critical discussions and helpful suggestions. This work was supported by the Kimmelman Center for Macromolecular Assemblies. Y.L. holds The Morton and Gladys Pickman professional chair in Structural Biology. T.S. is the incumbent of the Monroy-Marks Research Fellow Chair.

REFERENCES

(1) Akke, M. Conformational dynamics and thermodynamics of protein-ligand binding studied by NMR relaxation. *Biochem. Soc. Trans.* **2012**, *40*, 419−423.
(2) Liu, X.; Speckhard, D. C.; Shepherd, T. R.; Sun, Y. J.; Hengel, S. R.; Yu, L.; Fowler, C. A.; Gakhar, L.; Fuentes, E. J. Distinct roles for conformational dynamics in protein-ligand interactions. *Structure* **2016**, *24*, 2053−2066.
(3) Amaral, M.; Kokh, D. B.; Bomke, J.; Wegener, A.; Buchstaller, H. P.; Eggenweiler, H. M.; Matias, P.; Sirrenberg, C.; Wade, R. C.; Frech, M. Protein conformational flexibility modulates kinetics and thermodynamics of drug binding. *Nat. Commun.* **2017**, *8*, 2276.
(4) Ertekin, A.; Massi, F. *Understanding the Role of Conformational Dynamics in Protein−Ligand Interactions Using NMR Relaxation Methods*; Wiley Online Library, 2014; Vol. 3, pp 255−266.
(5) Solomentsev, G.; Diehl, C.; Akke, M. Conformational entropy of fk506 binding to fkbp12 determined by nuclear magnetic resonance relaxation and molecular dynamics simulations. *Biochemistry* **2018**, *57*, 1451−1461.
(6) Capdevila, D. A.; Braymer, J. J.; Edmonds, K. A.; Wu, H.; Giedroc, D. P. Entropy redistribution controls allostery in a metalloregulatory protein. *Proc. Natl. Acad. Sci. U.S.A.* **2017**, *114*, 4424−4429.
(7) Johansson, K. E.; Lindorff-Larsen, K. Structural heterogeneity and dynamics in protein evolution and design. *Curr. Opin. Struct. Biol.* **2018**, *48*, 157−163.
(8) Papaleo, E.; Saladino, G.; Lambrughi, M.; Lindorff-Larsen, K.; Gervasio, F. L.; Nussinov, R. The role of protein loops and linkers in conformational dynamics and allostery. *Chem. Rev.* **2016**, *116*, 6391−6423.
(9) Sato, K.; Li, C.; Salard, I.; Thompson, A. J.; Banfield, M. J.; Dennison, C. Metal-binding loop length and not sequence dictates structure. *Proc. Natl. Acad. Sci. U.S.A.* **2009**, *106*, 5616−5621.
(10) Murphy, P. M.; Bolduc, J. M.; Gallaher, J. L.; Stoddard, B. L.; Baker, D. Alteration of enzyme specificity by computational loop remodeling and design. *Proc. Natl. Acad. Sci. U.S.A.* **2009**, *106*, 9215−9220.
(11) Collis, A. V. J.; Brouwer, A. P.; Martin, A. C. R. Analysis of the antigen combining site: Correlations between length and sequence composition of the hypervariable loops and the nature of the antigen. *J. Mol. Biol.* **2003**, *325*, 337−354.
(12) Streaker, E. D.; Beckett, D. Ligand-linked structural changes in the Escherichia coli biotin repressor: The significance of surface loops for binding and allostery. *J. Mol. Biol.* **1999**, *292*, 619−632.
(13) Wang, L.; Rivera, E. V.; Benavides-Garcia, M. G.; Nall, B. T. Loop entropy and cytochrome c stability. *J. Mol. Biol.* **2005**, *353*, 719−729.
(14) Scalley-Kim, M.; Minard, P.; Baker, D. Low free energy cost of very long loop insertions in proteins. *Protein Sci.* **2003**, *12*, 197−206.
(15) Ladurner, A. G.; Fersht, A. R. Glutamine, alanine or glycine repeats inserted into the loop of a protein have minimal effects on stability and folding rates. *J. Mol. Biol.* **1997**, *273*, 330−337.
(16) Viguera, A.-R.; Serrano, L. Loop length, intramolecular diffusion and protein folding. *Nat. Struct. Biol.* **1997**, *4*, 939−946.
(17) Nagi, A. D.; Regan, L. An inverse correlation between loop length and stability in a four-helix-bundle protein. *Folding Des.* **1997**, *2*, 67−75.

DOI: 10.1021/acs.jpcb.8b09658
J. Phys. Chem. B 2018, 122, 10855−10860

(18) Dagan, S.; Hagai, T.; Gavrilov, Y.; Kapon, R.; Levy, Y.; Reich, Z. Stabilization of a protein conferred by an increase in folded state entropy. *Proc. Natl. Acad. Sci. U.S.A.* **2013**, *110*, 10628−10633.
(19) Gavrilov, Y.; Dagan, S.; Levy, Y. Shortening a loop can increase protein native state entropy. *Proteins* **2015**, *83*, 2137−2146.
(20) Towse, C.-L.; Akke, M.; Daggett, V. The dynameomics entropy dictionary: a large-scale assessment of conformational entropy across protein fold space. *J. Phys. Chem. B* **2017**, *121*, 3933−3945.
(21) Caro, J. A.; Harpole, K. W.; Kasinath, V.; Lim, J.; Granja, J.; Valentine, K. G.; Sharp, K. A.; Wand, A. J. Entropy in molecular recognition by proteins. *Proc. Natl. Acad. Sci. U.S.A.* **2017**, *114*, 6563−6568.
(22) Wand, A. J.; Sharp, K. A. Measuring entropy in molecular recognition by proteins. *Annu. Rev. Biophys.* **2018**, *47*, 41−61.
(23) Frederick, K. K.; Marlow, M. S.; Valentine, K. G.; Wand, A. J. Conformational entropy in molecular recognition by proteins. *Nature* **2007**, *448*, 325−329.
(24) Wang, T.; Frederick, K. K.; Igumenova, T. I.; Wand, A. J.; Zuiderweg, E. R. P. Changes in calmodulin main-chain dynamics upon ligand binding revealed by cross-correlated NMR relaxation measurements. *J. Am. Chem. Soc.* **2005**, *127*, 828−829.
(25) Zidek, L.; Novotny, M. V.; Stone, M. J. Increased protein backbone conformational entropy upon hydrophobic ligand binding. *Nat. Struct. Biol.* **1999**, *6*, 1118−1121.
(26) Sharp, K. A.; O'Brien, E.; Kasinath, V.; Wand, A. J. On the relationship between NMR-derived amide order parameters and protein backbone entropy changes. *Proteins* **2015**, *83*, 922−930.
(27) Stefani, M.; Taddei, N.; Ramponi, G. Insights into acylphosphatase structure and catalytic mechanism. *Cell. Mol. Life Sci.* **1997**, *53*, 141−151.
(28) Fusco, G.; De Simone, A.; Hsu, S.-T. D.; Bemporad, F.; Vendruscolo, M.; Chiti, F.; Dobson, C. M. (1)H, (1)(3)C and (1)(5) N resonance assignments of human muscle acylphosphatase. *Biomol. NMR Assignments* **2012**, *6*, 27−29.
(29) Pastore, A.; Saudek, V.; Ramponi, G.; Williams, R. J. P. Three-dimensional structure of acylphosphatase. Refinement and structure analysis. *J. Mol. Biol.* **1992**, *224*, 427−440.
(30) Lipari, G.; Szabo, A. Model-free approach to the interpretation of nuclear magnetic-resonance relaxation in macromolecules .2. analysis of experimental results. *J. Am. Chem. Soc.* **1982**, *104*, 4559−4570.
(31) Lipari, G.; Szabo, A. Model-free approach to the interpretation of nuclear magnetic-resonance relaxation in macromolecules .1. theory and range of validity. *J. Am. Chem. Soc.* **1982**, *104*, 4546−4559.
(32) Clore, G. M.; Szabo, A.; Bax, A.; Kay, L. E.; Driscoll, P. C.; Gronenborn, A. M. Deviations from the simple 2-parameter model-free approach to the interpretation of n-15 nuclear magnetic-relaxation of proteins. *J. Am. Chem. Soc.* **1990**, *112*, 4989−4991.
(33) Clore, G. M.; Driscoll, P. C.; Wingfield, P. T.; Gronenborn, A. M. Analysis of the backbone dynamics of interleukin-1-beta using 2-dimensional inverse detected heteronuclear n-15-h-1 nmr-spectroscopy. *Biochemistry* **1990**, *29*, 7387−7401.
(34) Li, Z.; Raychaudhuri, S.; Wand, A. J. Insights into the local residual entropy of proteins provided by NMR relaxation. *Protein Sci.* **1996**, *5*, 2647−2650.
(35) Akke, M.; Skelton, N. J.; Kordel, J.; Palmer, A. G.; Chazin, W. J. NMR order parameters and free-energy - an analytical approach and its application to cooperative Ca2+ binding by calbindin-D(9k). *J. Am. Chem. Soc.* **1993**, *32*, 9832−9844.
(36) Yang, D.; Kay, L. E. Contributions to conformational entropy arising from bond vector fluctuations measured from NMR-derived order parameters: Application to protein folding. *J. Mol. Biol.* **1996**, *263*, 369−382.
(37) Mandel, A. M.; Akke, M.; Palmer, A. G., III Backbone dynamics of escherichia-coli ribonuclease hi - correlations with structure and function in an active enzyme. *J. Mol. Biol.* **1995**, *246*, 144−163.
(38) Prompers, J. J.; Brüschweiler, R. General framework for studying the dynamics of folded and nonfolded proteins by NMR relaxation spectroscopy and MD simulation. *J. Am. Chem. Soc.* **2002**, *124*, 4522−4534.
(39) O'Brien, E. S.; Wand, A. J.; Sharp, K. A. On the ability of molecular dynamics force fields to recapitulate NMR derived protein side chain order parameters. *Protein Sci.* **2016**, *25*, 1156−1160.
(40) Kasinath, V.; Sharp, K. A.; Wand, A. J. Microscopic insights into the nmr relaxation-based protein conformational entropy meter. *J. Am. Chem. Soc.* **2013**, *135*, 15092−15100.
(41) Koller, A. N.; Schwalbe, H.; Gohlke, H. Starting structure dependence of NMR order parameters derived from MD simulations: Implications for judging force-field quality. *Biophys. J.* **2008**, *95*, L04−L06.
(42) Liu, Q.; Shi, C.; Yu, L.; Zhang, L.; Xiong, Y.; Tian, C. General order parameter based correlation analysis of protein backbone motions between experimental NMR relaxation measurements and molecular dynamics simulations. *Biochem. Biophys. Res. Commun.* **2015**, *457*, 467−472.
(43) Palmer, A. G.; Grey, M. J.; Wang, C. Solution NMR spin relaxation methods for characterizing chemical exchange in high-molecular-weight systems. *Methods Enzymol.* **2005**, *394*, 430−465.
(44) Palmer, A. G.; Kroenke, C. D.; Loria, J. P. Nuclear magnetic resonance methods for quantifying microsecond-to-millisecond motions in biological macromolecules. *Methods Enzymol.* **2001**, *339*, 204−238.
(45) Hansen, D. F.; Vallurupalli, P.; Kay, L. E. An improved 15N relaxation dispersion experiment for the measurement of millisecond time-scale dynamics in proteins. *J. Phys. Chem. B* **2008**, *112*, 5898−5904.
(46) Li, D.-W.; Brüschweiler, R. A dictionary for protein side-chain entropies from NMR order parameters. *J. Am. Chem. Soc.* **2009**, *131*, 7226−7227.
(47) Baxa, M. C.; Haddadian, E. J.; Jumper, J. M.; Freed, K. F.; Sosnick, T. R. Loss of conformational entropy in protein folding calculated using realistic ensembles and its implications for NMR-based calculations. *Proc. Natl. Acad. Sci. U.S.A.* **2014**, *111*, 15396−15401.
(48) Baxa, M. C.; Haddadian, E. J.; Jha, A. K.; Freed, K. F.; Sosnick, T. R. Context and force field dependence of the loss of protein backbone entropy upon folding using realistic denatured and native state ensembles. *J. Am. Chem. Soc.* **2012**, *134*, 15929−15936.
(49) Numata, J.; Knapp, E.-W. Balanced and bias-corrected computation of conformational entropy differences for molecular trajectories. *J. Chem. Theory Comput.* **2012**, *8*, 1235−1245.
(50) Solomentsev, G. Y.; English, N. J.; Mooney, D. A. Effects of external electromagnetic fields on the conformational sampling of a short alanine peptide. *J. Comput. Chem.* **2012**, *33*, 917−923.
(51) Harpole, K. W.; Sharp, K. A. Calculation of configurational entropy with a boltzmann-quasiharmonic model: the origin of high-affinity protein-ligand binding. *J. Phys. Chem. B* **2011**, *115*, 9461−9472.
(52) Diehl, C.; Genheden, S.; Modig, K.; Ryde, U.; Akke, M. Conformational entropy changes upon lactose binding to the carbohydrate recognition domain of galectin-3. *J. Biomol. NMR* **2009**, *45*, 157−169.
(53) Li, D.-W.; Showalter, S. A.; Brüschweiler, R. Entropy localization in proteins. *J. Phys. Chem. B* **2010**, *114*, 16036−16044.
(54) Li, D. W.; Brüschweiler, R. In silico relationship between configurational entropy and soft degrees of freedom in proteins and peptides. *Phys. Rev. Lett.* **2009**, *102*, 118108.
(55) Meirovitch, E.; Shapiro, Y. E.; Polimeno, A.; Freed, J. H. Protein dynamics from NMR: The slowly relaxing local structure analysis compared with model-free analysis. *J. Phys. Chem. A* **2006**, *110*, 8366−8396.
(56) Berezovsky, I. N.; Chen, W. W.; Choi, P. J.; Shakhnovich, E. I. Entropic stabilization of proteins and its proteomic consequences. *PLoS Comput. Biol.* **2005**, *1*, e47.

DOI: 10.1021/acs.jpcb.8b09658
J. Phys. Chem. B 2018, 122, 10855−10860